Cylinders with Elliptic Cross-Section: Wake Stability with Variation in Angle of Incidence

Gregory J. SHEARD

Fluids Laboratory for Aeronautical and Industrial Research (FLAIR), and
Monash University Biomedical Engineering Technology Alliance (MuBeta),
Department of Mechanical Engineering, Monash University, VIC 3800, Australia.
Corresponding author: Greg.Sheard@eng.monash.edu.au

Abstract. Direct numerical simulation and a stability analysis are employed to investigate the relationship between incidence angle (α) and three-dimensional wake stability for cylinders with an elliptical cross-section. An ellipse with a major to minor axis ratio of 2.0 is used, and incidence angles between the major axis and flow direction are varied from $\alpha = 0°$ to 30°. Reynolds numbers up to $Re = 500$ were considered based on the minor-axis dimension. Incidence angles were varied to break the wake centreline symmetry, which permitted an investigation into the subsequent availability, stability, and symmetry of three-dimensional instability modes in the wake.
At zero incidence angle, two synchronous modes with symmetries consistent with Mode B behind a circular cylinder are identified. One resembles Mode B in structure, and is neutrally stable at $Re = 419.7$ with a spanwise wavelength $\lambda_z/d = 0.825$. The other is neutrally stable at $Re = 283.1$ with $\lambda_z/d = 2.40$. For $Re \lesssim 250$ at longer wavelengths ($\lambda_z/d \approx 4.5$) a quasi-periodic mode is detected, but before it acquires a positive growth rate it is suppressed by shorter and longer-wavelength synchronous modes. Beyond $Re \approx 330$, evidence of a synchronous Mode A-type instability is observed with $\lambda_z/d \approx 4$.
With an increase in incidence angle, the proportion of wavelengths for which quasi-periodic modes are the fastest-growing instabilities reduce, and due to the increasing "bluffness" of the body, the growth rates increase across a wide range of spanwise wavelengths.

Key words: Instability, wake, elliptic cylinder, incidence angle, Floquet stability analysis, spectral element method.

1. Introduction

Recent studies have shown different bifurcation scenarios for three-dimensional transitions in cylinder wakes, depending on the wake symmetry [4, 22]. Cylinders with cross-sections which are symmetric about wake centreline exhibit correspondingly symmetrical wakes, in a time-averaged sense. Cylinders that have a cross-section asymmetrical about their centreline exhibit an asymmetrical time-averaged wake.
Cylinders that produce a wake comprising an approximately single-file line of alternating-sign vortices (e.g., the classic von Kármán vortex street behind a circular cylinder) are considered favorable for application of a linear Floquet stability analysis [3]. This is due to the wake adopting a perfect time-periodicity. However, cylinders which create wakes comprising widely-spaced vortices are typically unsuitable for such a stability analysis. These wakes tend to develop secondary shear layer instabilities further downstream, which introduce incommensurate wake frequencies that

destroy the periodicity of the wake. Examples of favorable cylinder cross-sections include circles [3], squares [14, 4], elongated bodies [15], and slender rings [20], whereas unfavorable sections include plates and ellipses aligned normal to the flow [9, 25]. The primary geometric feature influencing this categorization is the "bluffness" (ratio of cross-section height to width) of the cylinder in relation to the direction of flow. Cross-sections with high height-to-width ratios tend to produce unfavorable wakes, and those with lower height-to-width ratios tend to produce favorable wakes.

Favorable cylinders with a symmetrical cross-section (such as a circular cylinder) have been conclusively shown [4] to produce two-dimensional wakes unstable to synchronous three-dimensional Mode A and B-type instabilities, as well as a quasi-periodic instability characterized by a complex-conjugate pair of Floquet multipliers. Cylinders which lack symmetry about the centreline tend to produce wakes which are unstable to a true subharmonic mode (e.g., Mode C in the wake behind rings [20, 22]) instead of a quasi-periodic mode.

To the author's knowledge, the only studies to have systematically altered a wake centreline symmetry while monitoring the stability of a wake to three-dimensional instability modes are [20, 21, 22] for the wakes behind slender rings of various thickness. However, a ring only *approaches* a symmetric body (a circular cylinder) as the aspect ratio (diameter ratio of ring to its cross-section) approaches infinity. In this study, an elliptical cylinder will be used to target this problem, with variation in incidence angle providing a continuous means by which centreline symmetry can be broken.

2. Previous Elliptic Cylinder Studies

Elliptic cylinders have received a substantial amount of attention in the literature due to their widespread fluid mechanics applications. Elliptical cylinders aligned perpendicular to the oncoming flow were investigated analytically [23], where streamline patterns at the low-Reynolds-number limit were obtained, and more recently [9] using a spectral-element method, where a secondary instability was detected in the far wake, breaking the periodicity of two-dimensional Kármán wake.

Numerical studies were employed [10, 13] to investigate the flow around inclined impulsively started elliptic cylinders. They detected unsteady flow at $Re = 60$ and 200 for $\alpha = 30°$ and 45°, and steady flow at $Re = 15$ and 30.

The analogy between an elliptic cylinder in a channel and platelets moving in a blood vessel motivated numerical studies in which a cylinder was free to migrate in the flow direction [28], or free to translate and rotate throughout the channel [24]. In [28], steady-state solutions were obtained, and forces and moments on the cylinder were recorded, and in [24], the time-evolution of the position and orientation were obtained based on a flow solution in the low-Reynolds-number limit.

Unsteady flows over inclined elliptic cylinders have been considered [1, 2]. In those studies, the Reynolds number ranged between $10^2 \leq Re \leq 5000$, and Strouhal-Reynolds number trends and force measurements were reported. They drew favorable comparisons with inviscid flow solutions at higher Reynolds numbers, and reported a momentary negative lift shortly after the impulsive start of the fluid motion.

Another study [5] motivated by an engineering application employed Particle Image Velocimetry (PIV [8, 7]) to measure the near-wake velocity field behind an elliptic

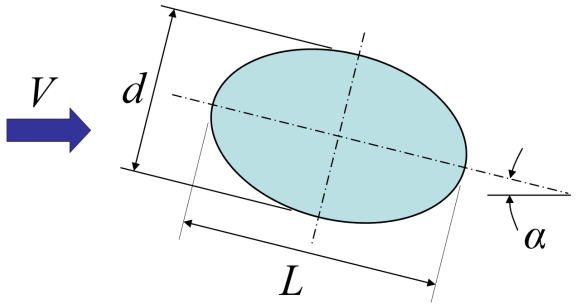

Figure 1. Schematic diagram showing the flow system under investigation. In this study, L was maintained at $2d$.

cylinder close to a free surface. That study recorded only time-averaged velocity fields.

While one anticipates the development of laminar and then turbulent three-dimensional flows through Reynolds numbers $O(10^2) \lesssim Re \lesssim O(10^3)$, two-dimensional numerical studies have been attempted for Reynolds numbers $3 \times 10^3 \leq Re \leq 10^4$ [11, 12]. An attempt at three-dimensional simulation of the near wake of an elliptic cylinder at $Re = 1.35 \times 10^4$ has also been reported [6]. Their results compared favorably to wind tunnel measurements, though discrepancies in wake width were found.

As this review has shown, surprisingly little attention has been afforded to the laminar three-dimensional transition regime for elliptic cylinders. This study will examine this regime in detail, and intends to firstly provide a clear understanding of the two-dimensional dynamics and three-dimensional stability of a $2:1$ elliptic cylinder aligned with the flow, before investigating the variation in wake stability with incidence angle.

3. Methodology

A two-dimensional circular cylinder with an elliptical cross-section (major to minor axis ratio of 2) is used for this investigation. The cylinder orientation and relevant nomenclature is shown in figure 1. A symmetric flow about the wake centreline is produced by aligning the major axis of the ellipse with the flow direction, and non-symmetrical cases being produced by inclining the cylinder at an incidence angle (α) to the oncoming flow. For consistency with previous studies, a Reynolds number is defined $Re = Vd/\nu$, based on the fluid kinematic viscosity ν, the freestream velocity V, and the *minor* axis dimension d of the cylinder cross-section.

A third-order time accurate two-dimensional spectral-element method [17, 18, 19, 16] is employed for this study, and three-dimensional wake stability is investigated using a Floquet linear stability analysis technique. A set of meshes were generated to model the cylinders at different incidence angles. Each mesh comprised 770 spectral elements, which were concentrated in the wake region and in the vicinity of the cylinder. The distances between the centre of the cylinder and the inlet, transverse boundary, and downstream boundary were $15d$, $30d$ and $25d$, respectively, consistent with previous stability analysis studies of cylinder wakes [3, 20, 4].

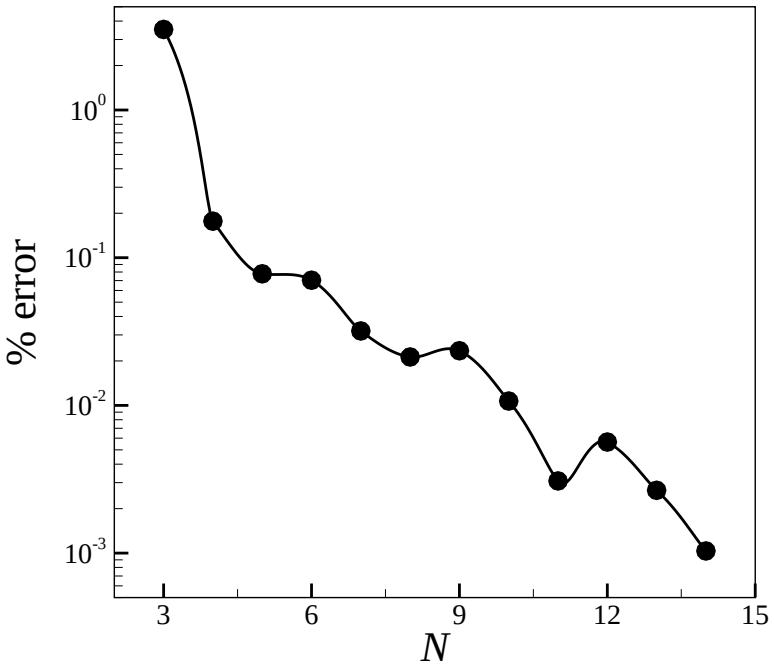

Figure 2. Percentage error in shedding frequency plotted against element polynomial degree N. Data was obtained at $Re = 300$ for an elliptical cylinder at zero angle of incidence.

A spatial resolution study was performed to determine the element polynomial degree (N) required to achieve accurate and resolved results. For the range $3 \leq N \leq 15$, Strouhal numbers ($St = fd/V$, where f is the shedding frequency) were recorded at $Re = 300$ for a cylinder with $\alpha = 0°$, and percent differences between each St and that at $N = 15$ were calculated. These are plotted in figure 2. Based on these findings, $N = 9$ was chosen for the computations to follow.

4. Two-Dimensional Wake Dynamics with Incidence Angle Variation

Before investigating the three-dimensional stability of the elliptic cylinder wakes, the time-periodic two-dimensional flow solutions were required. Strouhal numbers were recorded at Reynolds numbers $Re \lesssim 500$ for incidence angles $\alpha = 0°$, $5°$, $15°$ and $30°$. Further efforts were made to determine (using extrapolation to zero growth rate) the critical Reynolds and Strouhal numbers (Re_c and St_c, respectively) at the onset of the two-dimensional unsteady wake. These trends are plotted in figure 3. Curiously, a highly linear relationship exists between Re_c and St_c over this incidence angle range, with both parameters decreasing with an increase in incidence angle.

5. Three-Dimensional Stability at Zero Incidence Angle

At zero incidence angle, this elliptic cylinder is effectively a more streamlined equivalent of a circular cylinder, and therefore should experience a similar bifurcation scenario through the three-dimensional transition regime. In particular, instability

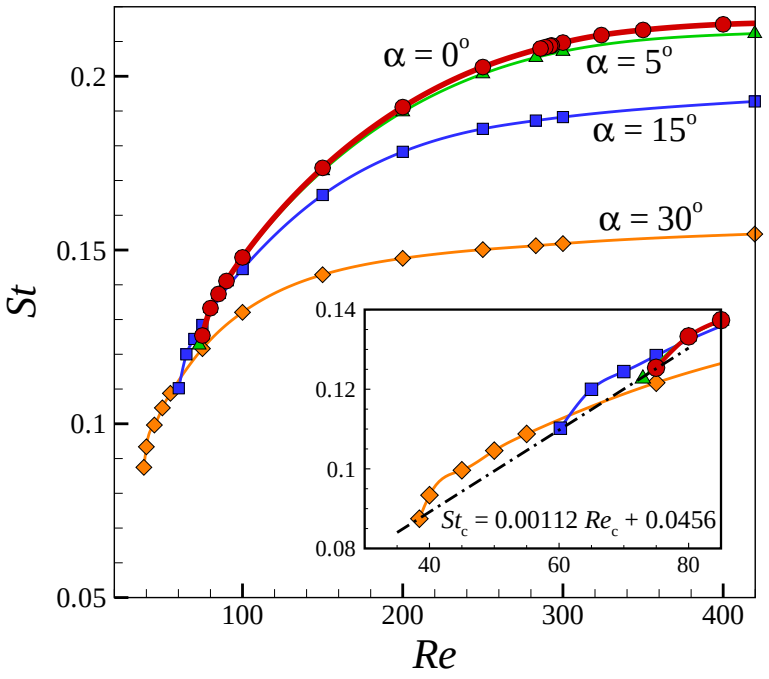

Figure 3. Strouhal number plotted against Reynolds number for elliptical cylinders at angles $\alpha = 0°$ (◯), 5° (△), 15° (□) and 30° (◇). Inset: A linear trend to the critical Reynolds and Strouhal numbers at the onset of unsteady flow for incidence angles $0° \leq \alpha \leq 30°$.

to synchronous (real) instability modes, and possibly a quasi-periodic (complex-conjugate) mode, is expected. Each mode may have unique symmetry, spanwise wavelength, and stability characteristics, and these may also differ from those found in the circular cylinder wake. Wake instabilities are known to scale on different wake features [27, 26], and it is likely that these scales will differ between the elliptic and circular cylinder wakes.

Floquet multiplier magnitudes ($|\mu|$) were obtained for a wide range of spanwise wavelengths and Reynolds numbers. Some of the data is plotted in figure 4 to illustrate the major findings of this analysis. The first mode to become unstable ($|\mu| > 1$) was found to be a synchronous mode with a symmetry consistent with the Mode B instability. This mode was neutrally stable at $Re = 283.1$ with a spanwise wavelength $\lambda_z/d = 2.40$. This and the following values were obtained by using high-order polynomial interpolation in both the Re and λ_z directions. Inspection of the perturbation field of this mode showed that it has a different structure to Mode B (see [3] for plots of a Mode B perturbation in the wake of a circular cylinder). Furthermore, the spanwise wavelength is approximately three times that of Mode B, so this study designates this mode as Mode B*. A streamwise vorticity contour plot obtained from the perturbation of this mode is shown in figure 5(a).

The second clearly defined mode to become unstable occurs at $Re = 419.7$ with $\lambda_z/d = 0.825$. This mode was identified as a Mode B-type instability, as it was consistent with Mode B for a circular cylinder in terms of structure, symmetry and spanwise wavelength. The structure of this mode is shown in figure 5(b).

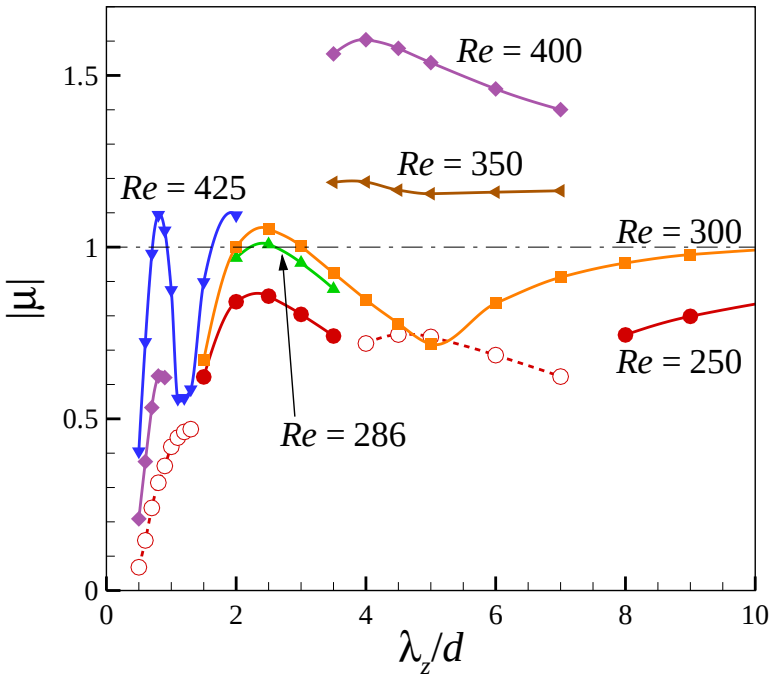

Figure 4. Floquet multiplier magnitudes plotted against spanwise wavelength for an elliptical cylinder at zero incidence angle. Filled symbols and solid lines denote real Floquet modes, whereas open symbols and dotted lines denote quasi-periodic Floquet modes. A dash-dotted line marks the neutral stability threshold at $|\mu| = 1$, and each data series are labelled with their corresponding Reynolds number.

The elliptic cylinder differs from the circular cylinder in that no Mode A-type instability is observed to cross the neutral stability threshold. At $Re \approx 330$, spanwise wavelengths $\lambda_z/d \gtrsim 2$ all have $|\mu| \gtrsim 1$, due to both the wide bandwidth of the now-unstable Mode B*, and the natural propensity for perturbations to exhibit $|\mu| \to 1$ behaviour as $\lambda_z/d \to \infty$. However, beyond $Re \approx 330$, a local maximum emerges in the $|\mu|$–λ_z/d trend at $\lambda_z/d \approx 4$. This wavelength is consistent with Mode A in a circular cylinder wake, and the structure and symmetry of the mode (see figure 5(c)) are also consistent. Hence Mode A makes a belated appearance in the stability scenario for a 2 : 1 elliptic cylinder.

Quasi-periodic multipliers were observed at a number of wavelengths, though they typically dominated at lower Reynolds numbers and did not become unstable. They were most prevalent up to $Re \approx 250$ with $\lambda_z/d \approx 4.5$, and up to $Re \approx 300$ with $\lambda_z/d \approx 1.2$. In each case, these local maxima corresponding to quasi-periodic mode branches were suppressed by faster-growing synchronous instabilities at each wavelength. The structure of the longer-wavelength quasi-periodic mode is shown in figure 5(d). This mode resembles Mode A in symmetry and structure, despite its Floquet multiplier containing an imaginary component.

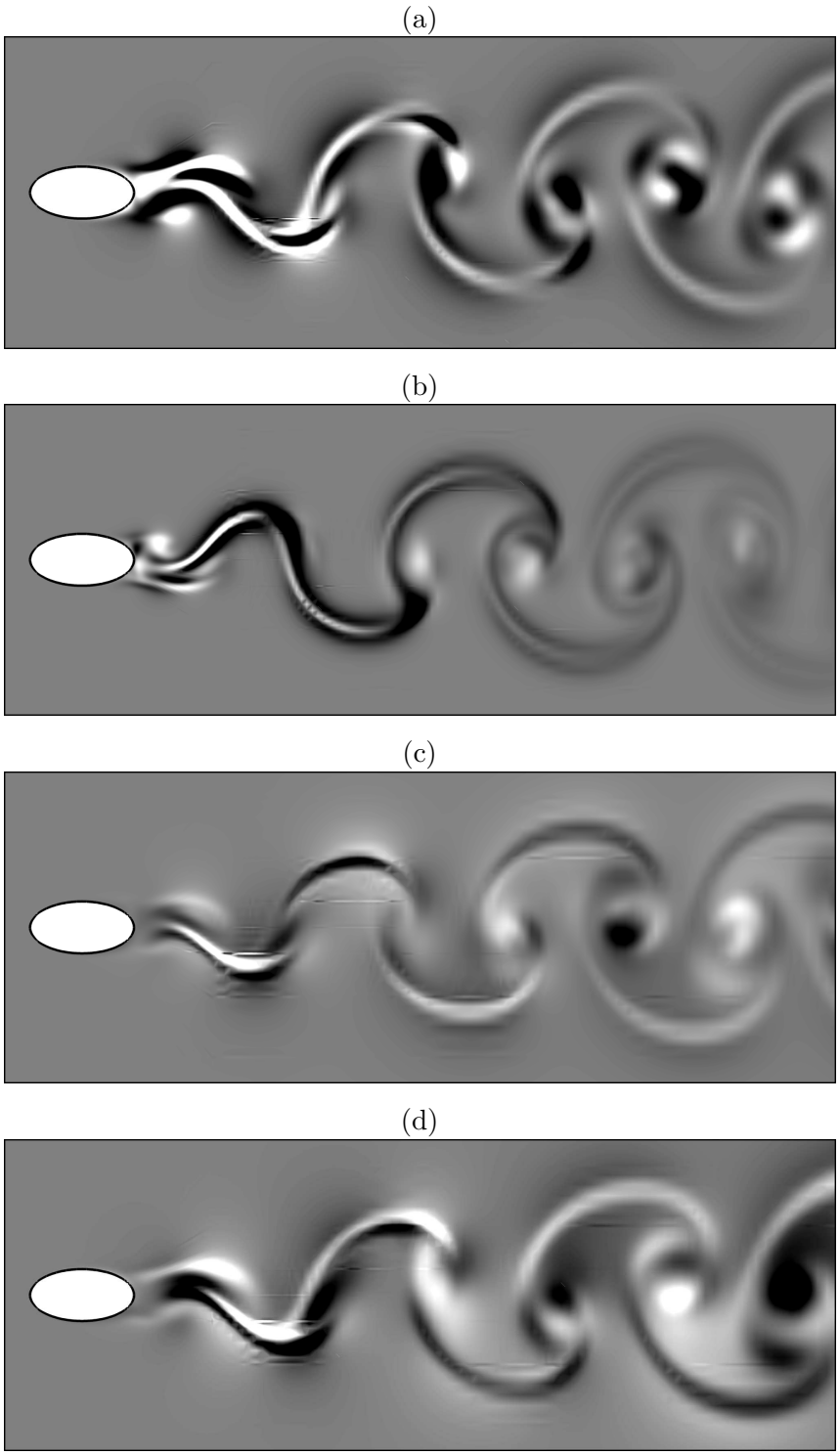

Figure 5. Plots of streamwise vorticity for the modes identified in the wake of an elliptical cylinder at zero incidence angle. (a-b) Neutrally stable synchronous modes with $\lambda_z = 2.40d$ at $Re = 283.1$, and $\lambda_z = 0.825d$ at $Re = 419.7$, respectively. (c) An unstable synchronous mode with $\lambda_z = 3.5d$ at $Re = 324$. (d) A stable quasi-periodic mode with $\lambda_z = 4.5d$ at $Re = 250$.

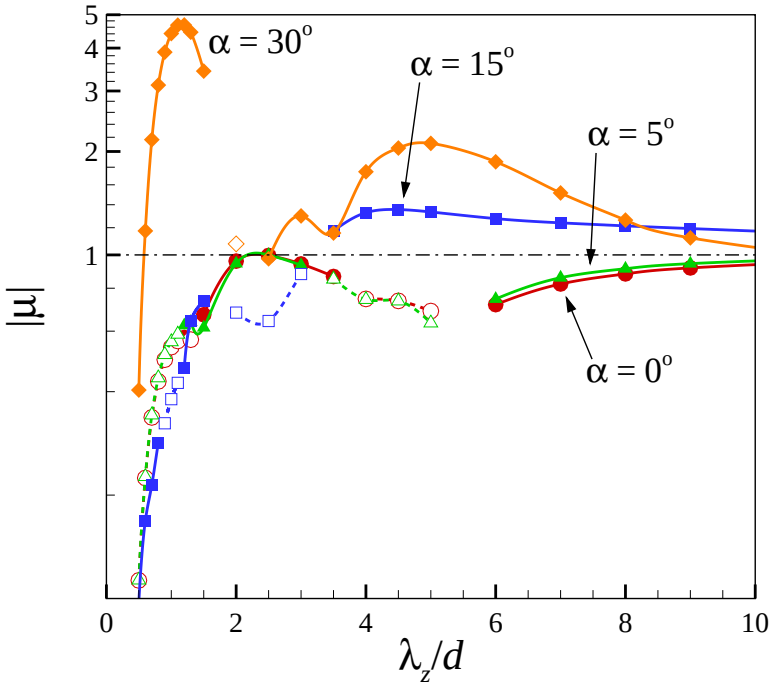

Figure 6. Floquet multiplier magnitudes plotted against spanwise wavelength for an elliptical cylinder at $Re = 283.1$. Wake stability was computed at various incidence angles, with symbols as per figure 3. Solid and open symbols denote synchronous and quasi-periodic modes, respectively, and a dash-dotted line denotes the neutral stability threshold.

6. Three-Dimensional Stability with Incidence Angle Variation

To assess the effect of variation of incidence angle on the wake stability, the stability of wakes at finite incidence angles was examined at $Re = 283.1$, corresponding to the predicted onset of three-dimensionality in the wake at zero incidence. The results of this study are plotted in figure 6. Two major conclusions can be drawn: firstly, the wakes become more unstable to three-dimensional perturbations as the angle of incidence is increased, and secondly, the proportion of wavelengths for which quasi-periodic modes are the fastest-growing instability decreases with an increase in incidence angle. This is in agreement with [4], who found that quasi-periodic modes are suppressed by time-averaged asymmetry about the wake centreline, which is increased in this study by increasing the incidence angle.
The fastest-growing wavelengths show substantial variation with incidence angle. At $\alpha = 15°$, $\lambda_z/d \approx 4.5$ is the fastest-growing wavelength, whereas at $\alpha = 30°$, it is $\lambda_z/d \approx 1.2$. The critical Reynolds numbers for the onset of three-dimensionality at these larger incidence angles is the subject of ongoing investigation.

7. Conclusions

The two-dimensional Strouhal-Reynolds number wake dynamics have been established for $Re \lesssim 500$ for a $2:1$ elliptic cylinder at a number of incidence angles over $0° \leq \alpha \leq 30°$. The critical Reynolds numbers for the onset of unsteady flow were

both found to decrease with an increase in incidence angle.
At zero incidence angle, the onset of three-dimensional flow is predicted to occur at $Re = 283.1$ through a synchronous bifurcation to a three-dimensional wake with spanwise wavelength $\lambda_z/d = 2.40$. This Mode B* instability has spatio-temporal symmetry consistent with Mode B for a circular cylinder, though the spanwise wavelength and structure of the mode are substantially different.
A genuine Mode B instability is predicted to emerge at $Re = 419.7$ with $\lambda_z/d = 0.825$, and evidence of unstable wavelengths with a mode structure consistent with a Mode A instability were found beyond $Re \approx 330$ with $\lambda_z/d \approx 4$.
With an increase in incidence angle a substantial increase in the growth rates of the instabilities was computed, corresponding to a reduction in the critical Reynolds number for the onset of three-dimensional flow. In addition, quasi-periodic modes were found to be gradually suppressed with an increase in incidence angle, corresponding to an increase in asymmetry of the time-averaged flow about the wake centreline. At $\alpha = 15°$, a mode with spanwise wavelength $\lambda_z/d \approx 4.5$ was the fastest-growing, while at $\alpha = 30°$, $\lambda_z/d \approx 1.2$ was the fastest-growing wavelength.

Acknowledgements

The author received salary as an Australian Postdoctoral Fellow under ARC Discovery Grant DP0555987 from the Australian Research Council. The computational resources of the Australian Partnership for Advanced Computing were utilized to complete this study, thanks to a time allocation under the Merit Allocation Scheme.

References

[1] H. M. Badr. Oscillating viscous flow over an inclined elliptic cylinder. *Ocean Engng.*, 21(4):401–426, 1994.

[2] H. M. Badr, S. C. R. Dennis, and S. Kocabiyik. Numerical simulation of the unsteady flow over an elliptic cylinder at different orientations. *Int. J. Numer. Meth. Fluids*, 37:905–931, 2001.

[3] D. Barkley and R. D. Henderson. Three-dimensional Floquet stability analysis of the wake of a circular cylinder. *J. Fluid Mech.*, 322:215–241, 1996.

[4] H. M. Blackburn and J. M. Lopez. On three-dimensional quasi-periodic Floquet instabilities of two-dimensional bluff body wakes. *Phys. Fluids*, 15(8):L57–L60, 2003.

[5] L. S. J. Daichin. Near-wake flow structure of elliptic cylinders close to a free surface: Effect of cylinder aspect ratio. *Exp. Fluids*, 36:748–758, 2004.

[6] M. R. Flynn and A. D. Eisner. Verification and validation studies of the time-averaged velocity field in the very near-wake of a finite elliptical cylinder. *Fluid Dyn. Res.*, 34:273–288, 2004.

[7] A. Fouras, J. Dusting, and K. Hourigan. A simple calibration technique for stereoscopic Particle Image Velocimetry. *Accepted for publication in Exp. Fluids.*, 2007.

[8] A. Fouras and J. Soria. Accuracy of out-of-plane vorticity measurements derived from in-plane velocity field data. *Exp. Fluids.*, 25:409–430, 1998.

[9] S. A. Johnson, M. C. Thompson, and K. Hourigan. Predicted low frequency structures in the wake of elliptical cylinders. *Euro. J. Mech. B/Fluids*, 23:229–239, 2004.

[10] H. J. Lugt and H. J. Haussling. Laminar flow past an abruptly accelerated elliptic cylinder at 45° incidence. *J. Fluid Mech.*, 65(4):711–734, 1974.

[11] M. T. Nair and K. Sengupta. Onset of asymmetry: Flow past circular and elliptic cylinders. *Int. J. Numer. Meth. Fluids*, 23:1327–1345, 1996.

[12] M. T. Nair and K. Sengupta. Unsteady flow past elliptic cylinders. *J. Fluids Struct.*, 11:555–595, 1997.

[13] V. A. Patel. Flow around the impulsively started elliptic cylinder at various angles of attack. *Comput. Fluids*, 9(4):435–462, 1981.

[14] J. Robichaux, S. Balachandar, and S. P. Vanka. Three-dimensional Floquet instability of the wake of a square cylinder. *Phys. Fluids*, 11(3):560–578, 1999.

[15] K. Ryan, M. C. Thompson, and K. Hourigan. Three-dimensional transition in the wake of bluff elongated cylinders. *J. Fluid Mech.*, 538:1–29, 2005.

[16] G. J. Sheard, K. Hourigan, M. C. Thompson, and T. Leweke. Flow around an impulsively arrested circular cylinder. *Under consideration for publication in Phys. Fluids*, 2007.

[17] G. J. Sheard, T. Leweke, and K. Hourigan. The vortex trajectories invoked by an arresting cylinder. In P. J. Witt & P. Schwarz, editor, *Proceedings of the Fifth International Conference on CFD in the Process Industries*, Hilton on the Park, Melbourne, Australia, 2006. Published by CSIRO Australia. ISBN: 0-643-09423-7 CD-ROM.

[18] G. J. Sheard and K. Ryan. The flow past particles driven by a pressure gradient in small tubes. In P. J. Witt & P. Schwarz, editor, *Proceedings of the Fifth International Conference on CFD in the Process Industries*, Hilton on the Park, Melbourne, Australia, 2006. Published by CSIRO Australia. ISBN: 0-643-09423-7 CD-ROM.

[19] G. J. Sheard and K. Ryan. Pressure-driven flow past spheres moving in a narrow tube. *Under consideration for publication in J. Fluid Mech.*, 2007.

[20] G. J. Sheard, M. C. Thompson, and K. Hourigan. From spheres to circular cylinders: The stability and flow structures of bluff ring wakes. *J. Fluid Mech.*, 492:147–180, 2003.

[21] G. J. Sheard, M. C. Thompson, and K. Hourigan. From spheres to circular cylinders: Non-axisymmetric transitions in the flow past rings. *J. Fluid Mech.*, 506:45–78, 2004.

[22] G. J. Sheard, M. C. Thompson, K. Hourigan, and T. Leweke. The evolution of a subharmonic mode in a vortex street. *J. Fluid Mech.*, 534:23–38, 2005.

[23] K. Shintani, A. Umemura, and A. Takano. Low-Reynolds-number flow past an elliptic cylinder. *J. Fluid Mech.*, 136:277–289, 1983.

[24] M. Sugihara-Seki. The motion of an elliptical cylinder in channel flow at low Reynolds numbers. *J. Fluid Mech.*, 257:575–596, 1993.

[25] M. C. Thompson, K. Hourigan, K. Ryan, and G. J. Sheard. Wake transition of two-dimensional cylinders and axisymmetric bluff bodies. *J. Fluids Struct.*, 22(6):793–806, 2006.

[26] M. C. Thompson, T. Leweke, and C. H. K. Williamson. The physical mechanism of transition in bluff body wakes. *J. Fluids Struct.*, 15:607–616, 2001.

[27] C. H. K. Williamson. Vortex dynamics in the cylinder wake. *Ann. Rev. Fluid Mech.*, 28:477–539, 1996.

[28] Y. Zhao and M. K. Sharp. Stability of elliptical cylinders in two-dimensional channel flow. *J. Biomech. Eng.*, 122:493–497, 2000.